FINAL REPORT ~ FHWA-OK-19-09

FEASIBILITY STUDY OF GRS SYSTEMS FOR BRIDGE ABUTMENTS IN OKLAHOMA: INFLUENCE OF FACING AND AGGREGATE FILL ON PERFORMANCE

Kianoosh Hatami, Ph.D., P.Eng.
Ridvan Doger, P.E, Ph.D. Candidate
Jérôme Boutin, M.Sc. Student

School of Engineering and Environmental Science (CEES)
The University of Oklahoma
Norman, Oklahoma

January 2020

FEASIBILITY STUDY OF GRS SYSTEMS FOR BRIDGE ABUTMENTS IN OKLAHOMA: INFLUENCE OF FACING AND AGGREGATE FILL ON PERFORMANCE

FINAL REPORT ~ FHWA-OK-19-09
ODOT SP&R ITEM NUMBER 2262

Submitted by:
Kianoosh Hatami, PhD, PEng
Ridvan Doger, PE, PhD Candidate
Jérôme Boutin, MSc Student

School of Civil Engineering and Environmental Science (CEES)
The University of Oklahoma

January 2020

TECHNICAL REPORT DOCUMENTATION PAGE

1. REPORT NO. FHWA-OK-19-09	2. GOVERNMENT ACCESSION NO.	3. RECIPIENT'S CATALOG NO.	
4. TITLE AND SUBTITLE FEASIBILITY STUDY OF GRS SYSTEMS FOR BRIDGE ABUTMENTS IN OKLAHOMA: INFLUENCE OF FACING AND AGGREGATE FILL ON PERFORMANCE		5. REPORT DATE Jan 2020	
		6. PERFORMING ORGANIZATION CODE	
7. AUTHOR(S) Kianoosh Hatami, Ridvan Doger and Jérome Boutin		8. PERFORMING ORGANIZATION REPORT	
9. PERFORMING ORGANIZATION NAME AND ADDRESS School of Engineering and Environmental Science (CEES) The University of Oklahoma 202 W Boyd St, Room 334, Norman, OK, USA		10. WORK UNIT NO.	
		11. CONTRACT OR GRANT NO. ODOT SPR Item Number 2262	
12. SPONSORING AGENCY NAME AND ADDRESS Oklahoma Department of Transportation Office of Research and Implementation 200 N.E. 21st Street, Room G18 Oklahoma City, OK 73105		13. TYPE OF REPORT AND PERIOD COVERED Final Report Oct 2017 - Dec 2019	
		14. SPONSORING AGENCY CODE	
15. SUPPLEMENTARY NOTES			

16. ABSTRACT

This document reports a study where load-bearing capacity, deformations and construction speed of different GRS abutment models were compared in the laboratory at full scale. Six 8 ft-high, instrumented abutment models were constructed inside an outdoor test station in order to study the influences that the choice of facing type, reinforcement spacing, fill aggregate and compaction effort could have on the structural performance and construction speed of GRS bridge abutments in the field. Results of the study show that even though facing is not considered a structural member in GRS bridge abutments, the choice of facing can influence their structural performance and construction speed. Models with large block facing tested in this study (i.e. Models #2 and #3) were easier to compact during construction and consistently showed smaller deformations relative to the control model (Model #1). The influence of backfill compaction on the structural performance of GRS abutments is also demonstrated and quantified. It is shown that models built using the recommended compaction effort (i.e. Models #4 and #5) are significantly stiffer relative to their settlement under the loading beam (simulating bridge load) and facing lateral deformation when compared to the control model with reduced compaction effort (Model #1).

17. KEY WORDS GRS-IBS, Bridge Abutments, Geosynthetics, Large Block Facing, Compaction, Soil Reinforcement		18. DISTRIBUTION STATEMENT No restrictions. This publication is available from the Office of Research and Implementation, Oklahoma DOT.	
19. SECURITY CLASSIF. (OF THIS REPORT) Unclassified	20. SECURITY CLASSIF. (OF THIS PAGE) Unclassified	21. NO. OF PAGES 44	22. PRICE N/A

Form DOT F 1700.7 (08/72)

SI* (MODERN METRIC) CONVERSION FACTORS

APPROXIMATE CONVERSIONS TO SI UNITS

SYMBOL	WHEN YOU KNOW	MULTIPLY BY	TO FIND	SYMBOL
LENGTH				
in	inches	25.4	millimeters	mm
ft	feet	0.305	meters	m
yd	yards	0.914	meters	m
mi	miles	1.61	kilometers	km
AREA				
in^2	square inches	645.2	square millimeters	mm^2
ft^2	square feet	0.093	square meters	m^2
yd^2	square yard	0.836	square meters	m^2
ac	acres	0.405	hectares	ha
mi^2	square miles	2.59	square kilometers	km^2
VOLUME				
fl oz	fluid ounces	29.57	milliliters	mL
gal	gallons	3.785	liters	L
ft^3	cubic feet	0.028	cubic meters	m^3
yd^3	cubic yards	0.765	cubic meters	m^3
NOTE: volumes greater than 1000 L shall be shown in m^3				
MASS				
oz	ounces	28.35	grams	g
lb	pounds	0.454	kilograms	kg
T	short tons (2000 lb)	0.907	megagrams (or "metric ton")	Mg (or "t")
TEMPERATURE (exact degrees)				
°F	Fahrenheit	5 (F-32)/9 or (F-32)/1.8	Celsius	°C
ILLUMINATION				
fc	foot-candles	10.76	lux	lx
fl	foot-Lamberts	3.426	candela/m^2	cd/m^2
FORCE and PRESSURE or STRESS				
lbf	poundforce	4.45	newtons	N
lbf/in^2	poundforce per square inch	6.89	kilopascals	kPa

APPROXIMATE CONVERSIONS FROM SI UNITS

SYMBOL	WHEN YOU KNOW	MULTIPLY BY	TO FIND	SYMBOL
LENGTH				
mm	millimeters	0.039	inches	in
m	meters	3.28	feet	ft
m	meters	1.09	yards	yd
km	kilometers	0.621	miles	mi
AREA				
mm^2	square millimeters	0.0016	square inches	in^2
m^2	square meters	10.764	square feet	ft^2
m^2	square meters	1.195	square yards	yd^2
ha	hectares	2.47	acres	ac
km^2	square kilometers	0.386	square miles	mi^2
VOLUME				
mL	milliliters	0.034	fluid ounces	fl oz
L	liters	0.264	gallons	gal
m^3	cubic meters	35.314	cubic feet	ft^3
m^3	cubic meters	1.307	cubic yards	yd^3
MASS				
g	grams	0.035	ounces	oz
kg	kilograms	2.202	pounds	lb
Mg (or "t")	megagrams (or "metric ton")	1.103	short tons (2000 lb)	T
TEMPERATURE (exact degrees)				
°C	Celsius	1.8C+32	Fahrenheit	°F
ILLUMINATION				
lx	lux	0.0929	foot-candles	fc
cd/m^2	candela/m^2	0.2919	foot-Lamberts	fl
FORCE and PRESSURE or STRESS				
N	newtons	0.225	poundforce	lbf
kPa	kilopascals	0.145	poundforce per square inch	lbf/in^2

*SI is the symbol for the International System of Units. Appropriate rounding should be made to comply with Section 4 of ASTM E380.
(Revised March 2003)

Table of Contents

List of Tables

List of Figures

1. Executive summary

This document reports a study where load-bearing capacity, deformations and construction speed of different GRS abutment models were compared in the laboratory at full scale. Six 8 ft-high, instrumented abutment models were constructed inside an outdoor test station in order to study the influences that the choice of facing type, reinforcement spacing, fill aggregate and compaction effort could have on the structural performance and construction speed of GRS bridge abutments in the field.

The first (control) model was built using the more commonly used, open-graded aggregate and hollow concrete masonry units (CMU) but with a reduced compaction effort (i.e. one pass) relative to the recommended practice of three passes of compactor equipment per backfill lift. Models #2 and #3 were built using much larger (i.e. 24" × 24" × 48") solid concrete blocks for their facing. Vertical spacing of geotextile reinforcement in Models #1 and #2 was kept at 8 inches, whereas it was increased to the limiting value of 12 inches in Model #3. Models #4 and #5 were built similar to Model #1 but with the recommended (i.e. increased) compaction effort to quantify anticipated improvements in their structural performance, and to compare their construction speed as a function of factors such as the presence of internal instrumentation and increased experience and training of the research team with the construction process, with anticipated benefits and implications to field construction. Finally, Model #6 was built similar to Model #4 but with a dense-graded aggregate, which is also allowed as an alternative type of fill in the FHWA guidelines.

Results of the study show that even though facing is not considered a structural member in GRS bridge abutments, the choice of facing can indeed influence their structural performance and construction speed. Models with large-block facing tested in this study (i.e. Models #2 and #3) were easier to compact during construction and consistently showed smaller deformations relative to the control model (Model #1). The influence of backfill compaction on the structural performance of GRS abutments is also demonstrated and quantified. It is shown that models built using the recommended compaction effort (i.e. Models #4 and #5) are significantly stiffer relative to their settlement under the loading beam (simulating bridge load) and facing lateral deformation when compared to the control model with reduced compaction effort (Model #1).

Among other findings of the study with field implications are the observation that repeat construction of GRS abutments by the same construction crew can significantly increase their construction speed, leading to further cost savings and reduced traffic disruptions, and that, several field projects that were surveyed during the course of this study have all shown satisfactory performance to date.

2. Introduction

The GRS-IBS technology has been developed primarily over the last decade through extensive support and promotion by the Federal Highway Administration as a viable and cost-effective bridge construction alternative to the conventional, deep-foundation abutment systems for local and county roads across the United States (FHWA 2012-16).

Results of an earlier study by the lead author's research team in Phase I of this project confirmed potential advantages of GRS-IBS bridges in Oklahoma, as have also been observed in many other states (Hatami *et al.* 2017). All GRS-IBS bridges that were constructed in Oklahoma during the first phase of the study have shown satisfactory performance to date, indicating that GRS-IBS can provide reliable and economical solutions to replace numerous structurally deficient and functionally obsolete bridges on local and county roads across Oklahoma. Many of these bridges are in dire need of repair or replacement in an economical manner and with minimum interruption of the local traffic.

While the economic advantage of GRS-IBS over the conventional abutment systems has been demonstrated in many projects in different states, it has been observed that their cost savings and reduced construction time could significantly diminish in the case of larger and taller GRS abutments (Hatami 2017).

In an effort to develop a potential solution, Mr. Shannon Sheffert, PE (Local Government Division Engineer at ODOT at the start of this project) and the lead author developed a plan to investigate the merits of using large concrete blocks (2' × 2' × 4') as the facing of GRS bridge abutments on local and county roads, anticipating that it would result in faster and less labor-intensive construction procedures leading to further cost savings. These blocks are already available through local suppliers in Oklahoma and other states. Therefore, one main purpose of this study was to test and quantify the anticipated advantages of large concrete blocks for the facing of GRS-IBS abutments through large-scale laboratory tests at OU and a possible field project.

Initially, the plan was to construct and load-test three full-scale (8' high), instrumented GRS abutment models at the OU outdoor test station in order to compare the construction speed and structural performance of models with larger blocks relative to that of a control GRS model with standard concrete masonry unit (CMU) facing. However, as the project progressed, the research team was able to build and test three additional full-scale models of GRS bridge abutments to also investigate the influences that compaction quality and aggregate type (i.e. dense-graded vs. open graded fills) could have on the anticipated structural performance and construction speed of these abutment systems.

This report provides details relative to the planning and preparations that were made to build and test the GRS abutment models; materials used and ancillary tests performed to determine their related properties; and construction, load testing and deconstruction of the models, followed by a discussion of the main results and conclusions. **Table 1** provides summary data on the abutment models tested in this study.

Table 1. Summary data on full-scale GRS abutment models tested in this study

Abutment Model Number	Backfill[1]	Facing[2]	Lift Thickness/ Reinforcement spacing (in.)	Compaction effort[3]	Target unit weight of backfill (pcf)	Backfill Friction angle (°)	Max. load applied (kips)	Max. vertical stress on the GRS fill (ksf)	FoS[4]	Max. settlement at the top of GRS fill (in.)	Constrained modulus[5], M (ksf)	Max. facing deformation (in.)	Construction effort (person-hours) Total	Construction effort (person-hours) Net[6]
1	O	CMU	8	1	100	46	353	70.6	17.7	6.2	1,127	0.79	123.5	74.5
2	O	LB	8	1	100	46	236	47.2	11.8	2.3	2,032	0.47	102.5	53.5
3	O	LB	12	1	100	46	202	40.4	10.1	2.2	1,818	0.33	82.5	33.5
4	O	CMU	8	3	105	46	221	44.2	11.1	1.7	2,574	0.23	99.0	50.2
5	O	CMU	8	3	105	46	252	50.4	12.6	1.7	2,846	0.22	27.0	27.0
6	D	CMU	8	3	105	45	259	51.8	13.0	1.6	3,108	0.23	53.6	26.9

Notes:
[1]O: Open graded; D: Dense graded (See Table 3 for more information)
[2]CMU: Concrete Masonry Units (Hollow concrete, 8" × 8" × 16"); LB: Large Blocks (Solid concrete, 24" × 24" × 48"), nominal dimensions
[3] Number of passes of model Rammer MS780 jumping jack (Chicago Pneumatic 2011) on each lift at full throttle
[4] Nominal value relative to design service load of 4 ksf (Adams et al. 2012a,b, 2018)
[5] Vertical stress/(settlement ÷ abutment height); calculated at maximum load as a lowerbound value
[6] Less the amount of time (effort) spent on model instrumentation (i.e. construction only)

3. Preliminary work in preparation for the project

Before this project could be started, several prerequisite subtasks had to be completed as described in the following sections.

4. Preparation of test facility and surrounding area

The test facility and its surrounding area had to be cleaned and cleared from significant amounts of soils, vegetation and debris from other earlier projects. The test box itself was full of hardened clayey soil from a previous project that needed to be excavated. At the same time, access to the test facility had been blocked by a large deposit of excavated subgrade soil from a recent roadway project next to the laboratory (**Figure 1**). The inside dimensions of the full-scale test box are 8 ft (width) × 9 ft (height) × 15 ft-6 inches (length).

Figure 1. (Left) Condition of the test station at the start of the project; (Right) Test box after cleaning and clearing in Task 1

5. Supplies and materials used for the project

Quantities of major material items necessary for the tests were determined and procured as shown in **Table 2**. These facing blocks and #2 Cover (open graded) aggregate are shown in **Figure 2**.

Table 2. Major materials and sensors used for the large-scale GRS models in this study

Material or Device	Application	Quantity	Specifications	Supplier
Aggregate	GRS Fill	50 tons each	AASHTO #89 or equivalent (#2 Cover - open graded) VDOT 21-A or equivalent (ODOT Type A - dense graded)	Dolese
Standard CMU Blocks	GRS Facing (16" × 8" × 8")	60 Full Blocks, 24 Half Blocks *(Read Note 1)*	Adams *et al.* (2012a,b)	Dolese
Large-Blocks	GRS Facing (48" × 24" × 24")	4 Full Blocks, 8 Half Blocks *(Read Note 2)*	NA	Dolese
Polypropylene Woven Geotextile	GRS Reinforcement, (4.8 k/ft × 4.8 k/ft ultimate tensile strength)	One Full Roll (5 yards x 100 yards)	Adams *et al.* (2012a,b)	TenCate Geosynthetics
Wirepots	Measuring displacements	6	PT101	Celesco
Wirepot Cables and Plastic Sleeves	Instrumentation	100 yards, each	NA	Miscellaneous
Angle beams, Anchor bolts and Fittings	Ancillary parts for instrumentation (e.g. to mount frontal wirepots against the GRS facing - see **Figures 8 and 9**)	Miscellaneous	NA	Miscellaneous
Load cells	Measuring applied load on GRS abutment	2 units	400-kip capacity	Interface
Earth pressure cells	Measuring earth pressure in GRS fill	Up to 5 units	Variable, VW	Geokon
Data loggers	Readout units for earth pressure cells	2 units	Models 8002-16 and 8021-1X	Geokon

Note 1: Need*ed due to the staggered pattern of the facing. Additional blocks were acquired throughout the project to replace damaged or broken blocks as necessary.*
Note 2: 24" × 24" × 24" 'half blocks' were used on the two sides of the central 'observation section'.

Figure 2. (Left) #2 Cover aggregate (open graded fill); (Right) Facing blocks stored near the test station

The comparison of aggregate gradations is given in **Table 3** below. Dolese 3/8" #2 Cover aggregate was used as the GRS fill as equivalent to AASHTO #89 aggregate. The ODOT Type A was used as equivalent for the VDOT 21-A.

Table 3. FHWA recommendations vs. actual aggregates used in the study

Sieve Size	FHWA Recommendation AASHTO #89 (Open graded) weight % passing	FHWA Recommendation VDOT 21-A (Dense graded) weight % passing	Actual Aggregate Used 3/8" #2 Cover (Open graded) weight % passing	Actual Aggregate Used ODOT Type A (Dense graded) weight % passing
2"	--	100	--	100
1"	--	94-100	--	98
½"	100	--	100	73
3/8"	90-100	63-72	90-100	--
No. 4	20-55	--	0-25	41
No. 8	0-15	--	0-5	--
No. 10	--	32-41	--	23
No. 16	0-10	--	--	--
No. 40	--	14-24	--	8
No. 50	0-5	--	--	--
No. 200	--	6-12	0-2	1

6. Development of GRS Model Instrumentation Plan and Calibration of Sensors

Preliminary stability analyses were carried out on eight-foot high abutment models using different computer programs to develop an instrumentation plan including locations of wire potentiometers (wirepots, WP) on the facing and within the GRS mass for the loading tests relative to the geometry of an anticipated slip plane. **Figure 3** shows screenshots of *TenCate MiraSlope®* and *TensarSoil®* analysis programs, respectively, which are two available computer programs from the industry. The models were analyzed using selected geotextile and geogrids properties with estimated slip planes as shown in **Figure 3**.
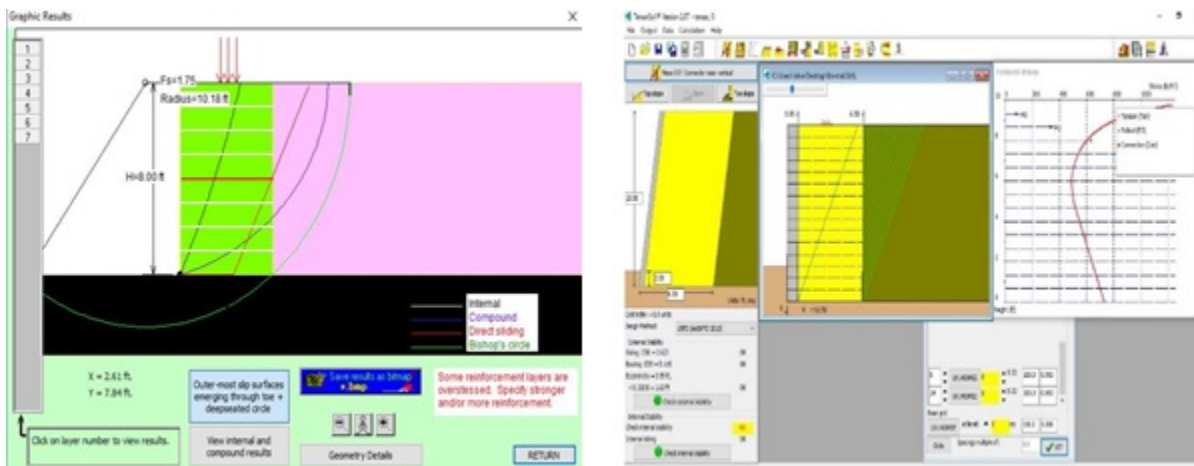
Figure 3. Screenshots of selected software programs for preliminary analysis of GRS abutment models: (Left) *TenCate MiraSlope®*; (Right) *TensarSoil®*

Based on the geometry of a potential slip plane under the applied load as predicted using the above stability analysis calculations, an instrumentation plan was developed for our first GRS model that included 16 wire potentiometers (WP) to measure reinforcement strains at four different elevations from the foundation slab (i.e. three at 27", four at 48" and 72" (each) and five at 87"), in addition to two (2) WPs to measure the settlements at the two opposite ends of the loading beam (simulating the bridge load) on the GRS abutment, and four (4) additional WPs to measure the lateral movement of GRS facing along its height (i.e. one at 39" and 63" (each) and two at 89" above the foundation slab). Additionally, three (3) earth pressure cells (EPCs) were used under the middle four feet (4') of the facing column (i.e. observation section), and two other within the reinforced mass at 44" and 82" above the foundation slab. Two different data-loggers (Geokon Models 8002-16 and 8021-1X) were used to record the EPC readings.

The surcharge load was applied approximately 24" away from the back of the facing block as a practically optimum location to instigate maximum deformation in the GRS mass while preventing merely local failure at the top by applying the load too close to the facing (**Figure 4**). It is worth noting that Abutment Model #5 did not include internal instrumentation because one particular objective for that model was to ascertain construction time and labor requirements as a simulated field abutment, which typically does not include internal sensors.

(a)

(b)

(c)

Figure 4. Cross-sectional views and instrumentation plans for GRS Abutment Models in this study: (a) Models #1, #4 and #6; (b) Model #2; and (c) Model #3. Dashed lines indicate estimated failure planes using friction angle values from DST.

Figure 5 shows a suggested schematic cross-sectional view of GRS abutments with large block facing alternative based on the geometry of the corresponding models that have been examined in this study and related construction notes from FHWA guidelines (Adams *et al.* 2012, 2018).
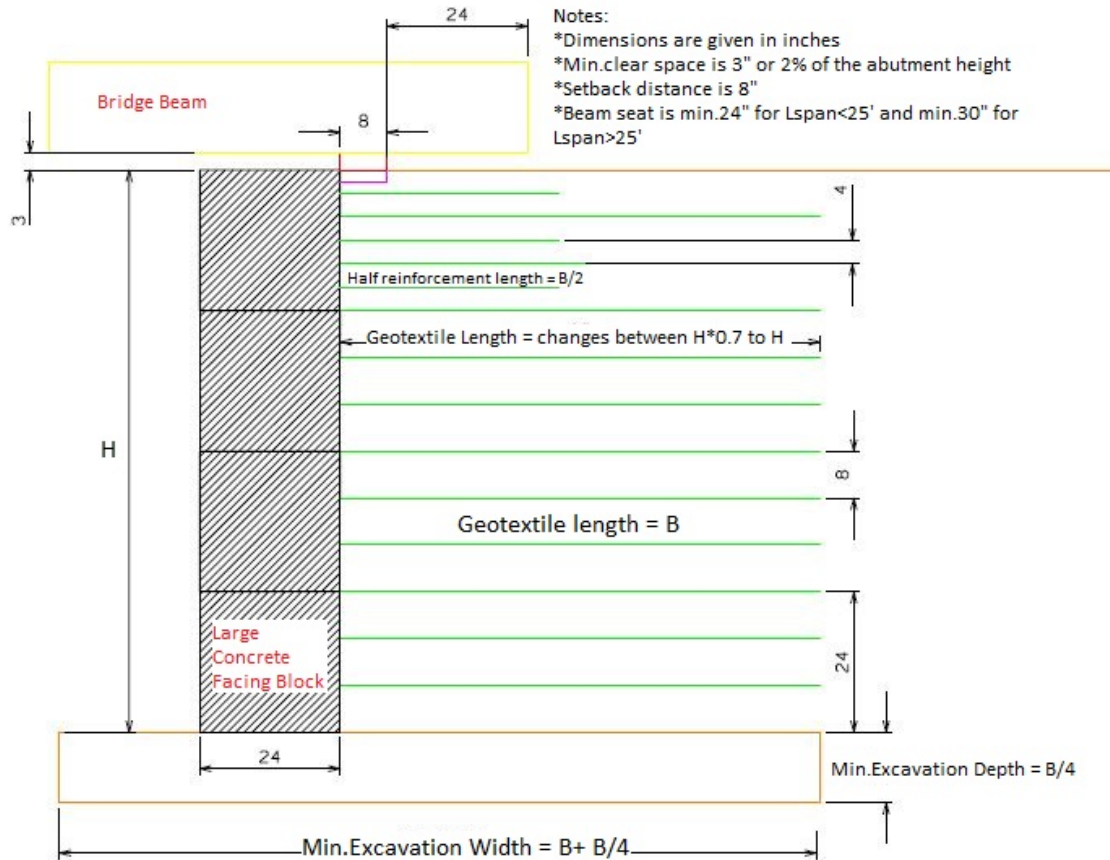
Figure 5. Suggested schematic cross-section of GRS Abutments with large concrete block facing with related construction notes from FHWA guidelines (Adams *et al.* 2012, 2018)

7. Material Testing and Instrumentation

a. GRS Fill Aggregate

A series of sieve analysis tests (ASTM C136) was carried out to verify the gradation of the GRS abutment backfill. Also, the compaction requirement for GRS fills is a minimum of 95% maximum dry density, Υ_{d_max}, as per AASHTO T-99 (Adams *et al.* 2012a,b). Therefore, a set of Proctor tests was carried out on aggregate samples in conformance with the ASTM D698 and D1557 test protocols, which yielded the values Υ_{d_max}= 100 pcf for the standard, and Υ_{d_max}= 105 pcf for the modified Proctor tests, correspondingly. The gradation results indicated that the open-graded, #2 Cover aggregate was

11

comparable to AASHTO #89 aggregate but with smaller percentages of finer particles. It also showed satisfactory agreement with the gradation provided by the supplier. Data from Proctor tests were used to calibrate a level of compaction effort (including the set intensity on the jumping jack and number of passes) for the abutment models using a 4' × 4' area in the outdoor test station. Additionally, large-scale direct shear tests (DST; ASTM D3080) were carried out on the GRS fill samples which yielded a friction angle value of approximately 44 degrees for the #2 Cover, which is within the range of values reported by Nicks *et al.* (2014) for different open graded aggregates. In contrast, friction angle values between 41 and 50 degrees were obtained for the dense graded aggregate (ODOT Type A).

b. Geotextile Reinforcement

Mirafi HP 570 was used for the geotextile reinforcement in the model abutments, which satisfies the FHWA strength requirements, including a minimum of 1,370 lb/ft strength at 2% strain in cross-machine direction (XD) as per the ASTM D4595 test protocol.

c. Geotextile-Aggregate Interface Tests

Large-scale pullout tests were carried out on geotextile specimens under different overburden pressures that included 12" and 18" of soil on the top of the specimen, and a third test with additional airbag surcharge of 1.5 psi on the top of the soil (**Figure 6**).

These tests were carried out to test the sensors and the data acquisition system (DAS) were in good operational conditions and to determine GRS aggregate-geotextile interface properties for future analysis. In these tests, actuator, DAS and earth pressure cell (EPC) data were collected simultaneously using separate computer stations and programs.

Figure 6. (Left) Geotextile specimen attached to the roller clamp of the pullout test actuator; (Right) EPC placed on the top of the sand before applying an airbag surcharge

d. Instrumentation of Geotextile Reinforcement with Wire Potentiometers

The reinforcement material was cut to size for all six GRS models, and stainless steel wires were cut and attached to selected layers according to the instrumentation plan using bolts and washers together with 2" × 2" geotextile patches for local reinforcement against rupture (**Figure 7**). The steel wires were passed through plastic tubes to protect them against gravel damage and they were attached to wire potentiometers (WP) that were mounted on the back of the test station to form wire extensometers to measure reinforcement displacements at selected locations.
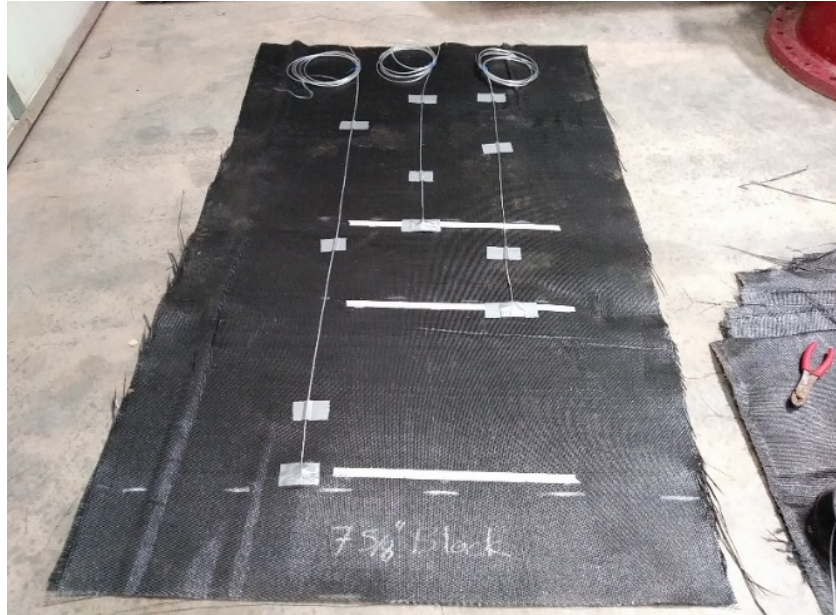

Figure 7. Example wirepot connections on a geotextile layer before installation in a GRS abutment model

8. Construction of GRS Abutment Models

Following the preparations and laboratory tests described in previous sections, different abutment models were constructed throughout the project period using the lift thickness and reinforcement spacing values reported in **Table 1.** During construction, labor requirements (in person-hours) were documented to help compare the construction speed of CMU-block (Control) models relative to that of large-block alternatives in future analysis.

In each model, additional shorter reinforcement layers were cut and placed underneath the loading beam (simulating the bridge abutment load) at 4" vertical spacing as per the FHWA guidelines (Adams *et al.* 2012, 2018). Afterwards, the loading assembly and ancillary instruments (i.e. loading beam, cylindrical loading extension blocks, load cells, and settlement WPs) were installed on the top of the GRS fill (**Figure 8**).

Abutment models #2 (**Figure 9**) and #3 were built similar to the control Model #1 except that large (24" × 24" × 48") blocks were for the facing. Also, similar to Model #1, the model facing was comprised of a 48"-wide instrumented, middle (observation) section flanked by two 24"-wide facing columns with separate reinforcement layers, and separated by full-height construction joints in the facing. However, in Model #1, the observation section was comprised of three 16"-long CMU blocks along the running length of the model whereas in Model #2, only one 48"-long large-block was sufficient for each level to construct this section of the model abutment.

Abutment Models #4 - #6 were constructed identical to Model #1 except that an increased compaction effort was applied to the GRS fill to investigate the influence of compaction energy and backfill unit weight on abutment performance (**Table 1**). Models #4 and #6 were instrumented internally with wire potentiometers (WP), but WPs were not used in Model #5 deliberately in order to simulate an actual construction procedure in the field more closely and be able to measure the required construction time more directly. Three compaction passes were used per each 8-in. lift to build Models #4 - #6 as recommended by the FHWA guidelines (Adams *et al.* 2018). Abutment Models #4 and #5 were built using the open-graded, 3/8" #2 Cover aggregate as backfill material. In contrast, the dense graded ODOT Type A aggregate was used in Model #6.

Two half (i.e. 24" × 24" × 24") blocks were placed on each side of the middle block to complete the length of the facing at each level. Also, as opposed to the first model where all three EPCs were installed in the same row under the 8"-thick CMU blocks, the EPCs in Model #2 were staggered across the width of the large-block with the objective to capture the non-uniform distribution of foundation pressure under the block. All three EPCs were checked and calibrated before installation. Also, the final sections (upper rows of blocks) in Models #2 and #3 were put in place using a large rental forklift.

It was observed that the much heavier blocks in Models #2 and #3 allowed for a significantly better compaction effort than the lighter CMU blocks, which had a tendency to move outward if the compaction equipment would get too close to the facing. This helped with both the speed and the quality of the GRS compaction in the region immediately behind the facing (i.e. uniformity of the unit weight relative to the rest of the GRS fill), which incidentally has a more significant influence on the facing deformation and the GRS performance as a whole relative to the remainder of the abutment fill.

It was also observed that compaction performance of the dense-graded ODOT Type A aggregate used in Model #6 was more sensitive to its moisture content relative to that of the #2 Cover aggregate used in earlier models, which was open graded and allowed water to drain more readily. The dense-graded aggregate was easier to compact when it was moist, but at the same time, it required additional care in the vicinity of the facing to prevent unintended movements of the CMU blocks. Even though such difference in

compaction behavior had been anticipated between the earlier open-graded and the newer dense-graded aggregates, the extra time and care that had to be exercised to construct the dense-graded fill served as a worthy reminder for field construction, suggesting that open-graded fill may be a more suitable option, especially for the lightweight CMU facing alternative.

9. Load Testing of GRS Abutment Models

After each abutment model was constructed and the loading assembly was fully set up on the GRS fill, the model was load tested in nominal 10-20 kPa surcharge increments until at least 2 inches of settlement was attained. The first model abutment ended up being loaded more than others with the intent to explore its stability and factor of safety relative to the recommended design load as discussed in the results section later in this report. A significant amount of load was applied to the model abutment to see if it would exhibit significant deformations and signs of internal slip planes within its GRS fill, in order to experimentally determine its ultimate load bearing capacity. However, it was observed that the GRS abutment remained stable even when the limits of the loading frame were reached.

Having the advantage of observations and data from the first GRS test, we chose to stay within safe load magnitudes in the following tests, while we still applied adequate amounts of load to be able to compare the performances of the GRS abutment models far beyond the serviceability limit recommended by the FHWA (i.e. ½ inch settlement at 25 kips of surcharge load). For each abutment model, after the applied load reached the target value, the model was unloaded gradually before the load was completely removed. The corresponding results and discussions are presented in **Section 12**.

Figure 8. (Left) Wire extensometers are attached to the facing of GRS Abutment Model #1 to measure its deformation at three different levels; (Right) Electric-hydraulic pump is attached to the loading assembly before the start of loading test

Figure 9. GRS Abutment Model #2 after surcharge loading test

10. Excavation and Post-Test Survey of GRS Abutment Models

After the load testing of each model was completed, the loading assembly was removed and the abutment model which included tightly spaced geotextile reinforcement layers and instrumentation was carefully excavated in thin layers. All instruments used on the models were inspected, removed and stored in the laboratory for future use. Meanwhile, settlements of selected lifts were measured relative to their initial target elevations during the excavation process. The abutment fill and the facing blocks were transported back to a nearby stockpile area using a front loader tractor for use in subsequent models (**Figures 10, 11 and 12**).

Figure 10. GRS Abutment Model #1 after load testing and removal of loading assembly: (Left) Scarp under the loading beam; (Right) Excavated fill above the top geotextile layer

Figure 11. (Left) Exhumed instrumented reinforcement layer during deconstruction of Abutment Model #1; (Right) Survey of maximum settlements along each reinforcement layer during deconstruction

Figure 12. (Top) Removal of large concrete facing blocks at the end of test; (Bottom left and right) Test box and nearby material storage area after testing and clearing out GRS Abutment Model #2

11. Sensor Check and Recalibration

After the conclusion of each test and once the deconstruction of the corresponding model had been completed, all instruments used were checked to examine their conditions in preparation for the construction of subsequent abutment models. The sensors were then recalibrated or repaired as necessary.

12. Results

Figures 13 through 18 show selected test results for GRS Abutment Models #1- #6, which are discussed separately in the following sections. **Table 4** summarizes different outcomes corresponding to the comparison of selected model performances to further help with the interpretation of the test results provided in this section.

Table 4. Outcomes from the comparison of different abutment models

Model Number	Outcome
1,4,5	Performance verification of control model with most commonly used materials
1,2	Influence of facing type
2,3	Influence of reinforcement spacing (S_v)
4,6	Influence of backfill type
1,4	Influence of compaction effort
4,5,6	Influence of the crew experience on construction speed

a. Load-settlement performance

Figure 13 and 14 shows load-settlement response of the beam representing bridge abutment for all six GRS models tested in this project, which were subjected to a minimum of 200-kip surcharge load. Comparison of data for the CMU facing model (i.e. Model #1) with those built using large facing blocks (Models #2 and #3) clearly show that large-block facing models were considerably stiffer than the CMU alternative, as had been postulated in the study. This means that the large-block facing can indeed add to the structural integrity and performance of GRS abutments relative to the more commonly used CMU blocks. For instance, data in **Figure 13** show that the measured settlement of the control model (Model #1) for the 25-kip design load is essentially the same as the limiting value of 0.5 inches as per the FHWA requirements. In comparison, the measured settlement for the large-block model with the same reinforcement spacing (Model #2) and under the same load magnitude is only 0.15 inches.

Results in **Figures 13** also show that both Abutment Models #2 and #3 (the latter model even with an increased reinforcement spacing of 12 inches) consistently maintain their superior load-bearing and deformation performance relative to that of Model #1 throughout the tests. At the maximum applied load level of 236.2 kips, the settlement of Model #2 at the top was only 2.2 inches as compared to 4.3 inches in Model #1 (i.e. a reduced amount of settlement by a factor of 2). This observation together with reduced construction time for large-block models relative to the CMU alternative as discussed in **Section 12d** indicates potential benefits of large facing block GRS abutments, which are worthy of field verification for more widespread adoption in practice. In the case of Model #3, potential cost savings were observed due to reduced construction time and amount of reinforcement material used in the abutment model.
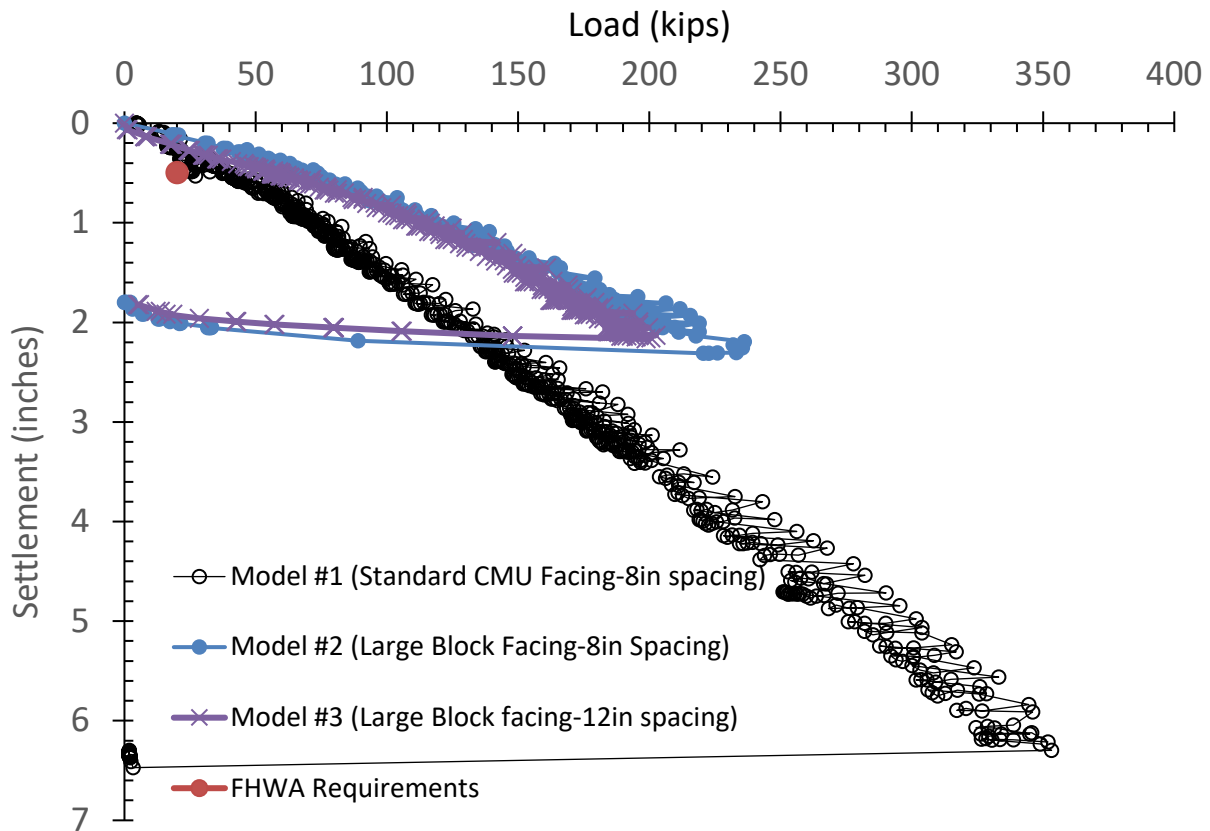
19

Figure 13. Load-settlement responses of GRS Abutment Models #1 - #3 (open-graded fill, reduced compaction effort of one pass/lift)

Results in **Figure 13** also indicate that for a mid-range load of 100 kips, GRS Model #1 (i.e. CMU facing with 8" geotextile spacing) showed the largest amount of settlement (i.e. 1.6"), whereas GRS Model #2 (i.e. large-block facing with 8" geotextile spacing) exhibited the lowest amount of settlement (i.e. 0.7"). GRS Model #3 (i.e. large-block facing with 12" geotextile spacing) showed only slightly larger settlement relative to GRS Model #2 (i.e. 0.8") and significantly lower settlement than Model #1, indicating that using large-block facing with increased reinforcement spacing could lead to an optimal design relative to both the performance and cost of bridge abutments.

Figure 14 shows a comparison of load-settlement results for Models #4 - #6, and show that given the range of settlements examined throughout the loading stage (i.e. relative to those shown in **Figure 13**), the performances of all three models are very similar to one another, with that of Model #6 (with a dense-graded fill) is slightly stiffer than those of Models #4 and #5 that were built with an open-graded fill. Models #4 and #5 were nominally identical except that Model #4 was internally instrumented. This could explain

why slightly larger settlements are observed for Model #4, possibly because the backfill was compacted with a slightly reduced amount of energy around the instruments relative to Model #5. This also suggests that the load-settlement responses of all other (instrumented) models could have been slightly stiffer had they not been instrumented internally (as is typically the case in the field).
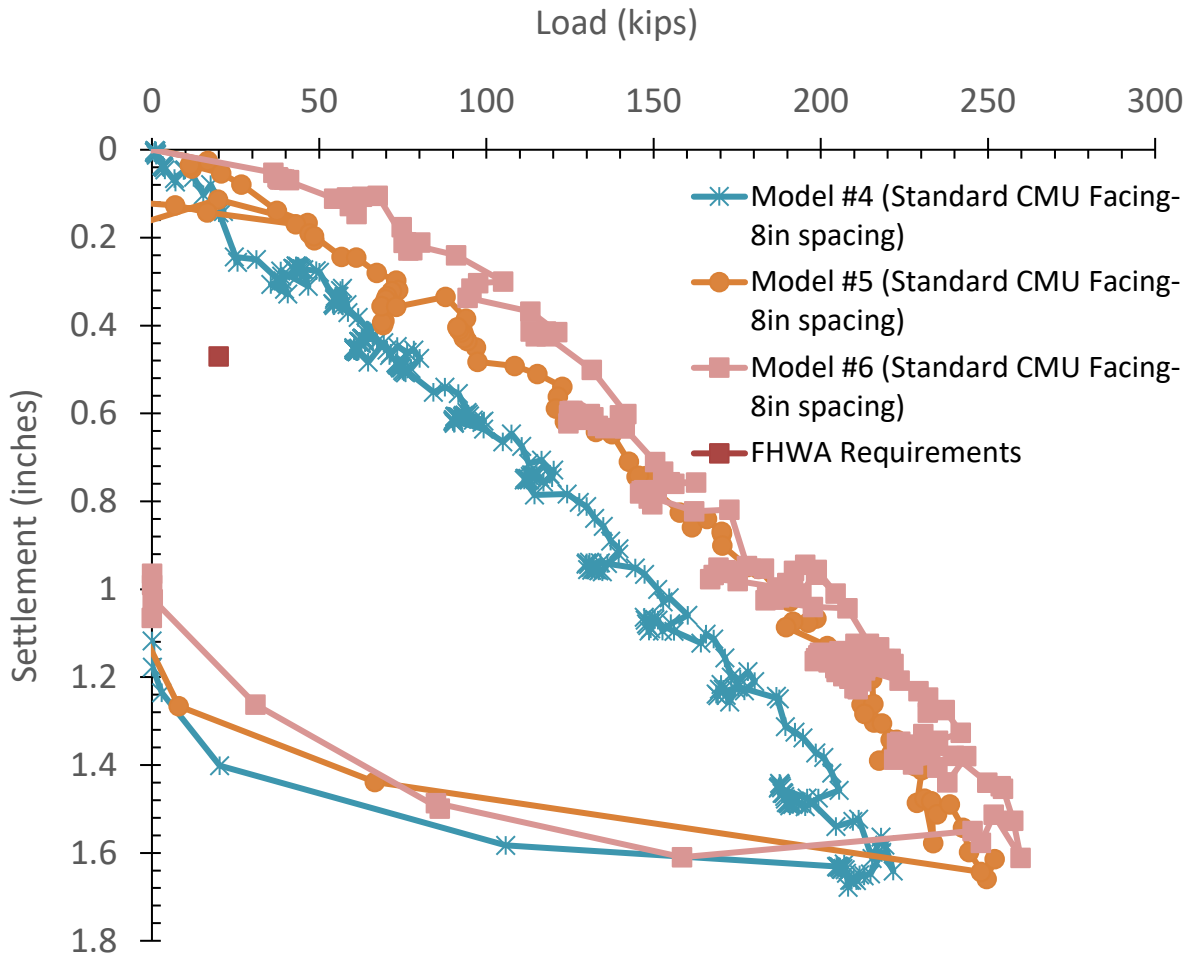

Figure 14. Load-settlement responses of GRS Abutment Models #4 - #6 (#4, #5: open-graded, and #6: dense-graded fills, all built with recommended compaction effort of three passes/lift)

Comparison of the results in **Figures 13 and 14** shows an important influence that backfill compaction effort could have (even for the more uniform open-graded fills) on the performance of GRS abutments. For instance, the measured amount of settlement in Model #1 (with reduced compaction effort) at 200 kips of surcharge load is approximately 3.2 inches. In comparison, the corresponding magnitudes of settlement (at 200 kips) in Models #4 - #6 are 1.4, 1.1, 1.0 inches, respectively, which are equal to,

or only slightly greater than, the limiting value of 1 inch (Adams *et al.* 2012, 2018) for the service load of 25 kips for the model abutments in this study.

The corresponding settlements for Models #2 and #3 with large facing blocks but reduced compaction effort are 1.8 and 2.1 inches, respectively. These results show that using large solid facing blocks could help counter the influence of reduced backfill compaction effort to a good extent, but adequate compaction is nevertheless necessary for GRS abutments to attain best performance. Models #4 - #6 that were built with recommended compaction effort (i.e. three passes of compactor per lift) all show significantly smaller settlements relative to Model #1, and to the FHWA recommended value even at significantly larger surcharge loads.

Figure 15 shows a complete set of surveyed deformations of the GRS fill at reinforcement levels during the deconstruction of Model #3 as a representative set of results. The data shown are mean values of manual measurements that were taken against the East- and Westside walls of the test box at each reinforcement layer. The theoretical Rankine slip plane using 44° friction angle for the granular fill is also shown in the figure. The friction angle value was determined using large-scale direct shear tests prior to the construction of GRS abutment models (**Section 7a**). Survey data in **Figure 15** show satisfactory agreement with the Rankine slip plane and the location of the loading beam at the GRS abutment surface. Results in **Figure 15** also indicate that GRS settlements at locations outside the pressure bulb of the loading beam are negligible. For instance, settlements taper off beyond 26" below the top of the GRS fill (i.e. deeper than elevation 63" above the foundation slab). These results, together with the significant factors of safety obtained for all abutment models examined, serve as another indication that GRS bridge abutments can indeed provide reliable supporting structures for roadway bridges without exhibiting noticeable settlements at intended service load levels.

b. Facing deformations

Figures 16 and 17 show facing lateral deformations of GRS abutment models in this study. Results in **Figure 16** show that lateral deformations of models with large concrete facing blocks were essentially the same regardless of reinforcement spacing used, and they were both significantly less than that of the control model with CMU facing. This indicates that use of large facing blocks could lead to a more economical design (through wider reinforcement spacing) while maintaining the same performance level, and it could help make the GRS bridge abutment alternative more economically attractive for local road projects in different states.
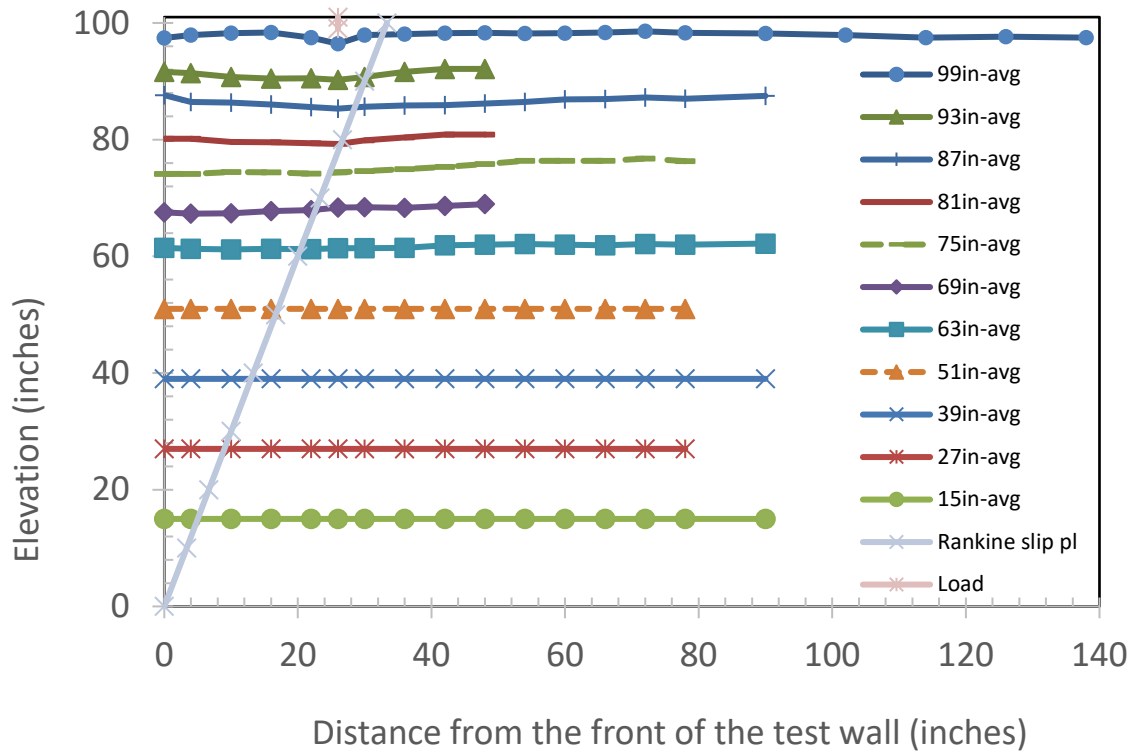
Figure 15. Settlement data at different reinforcement levels in GRS Abutment Model #3
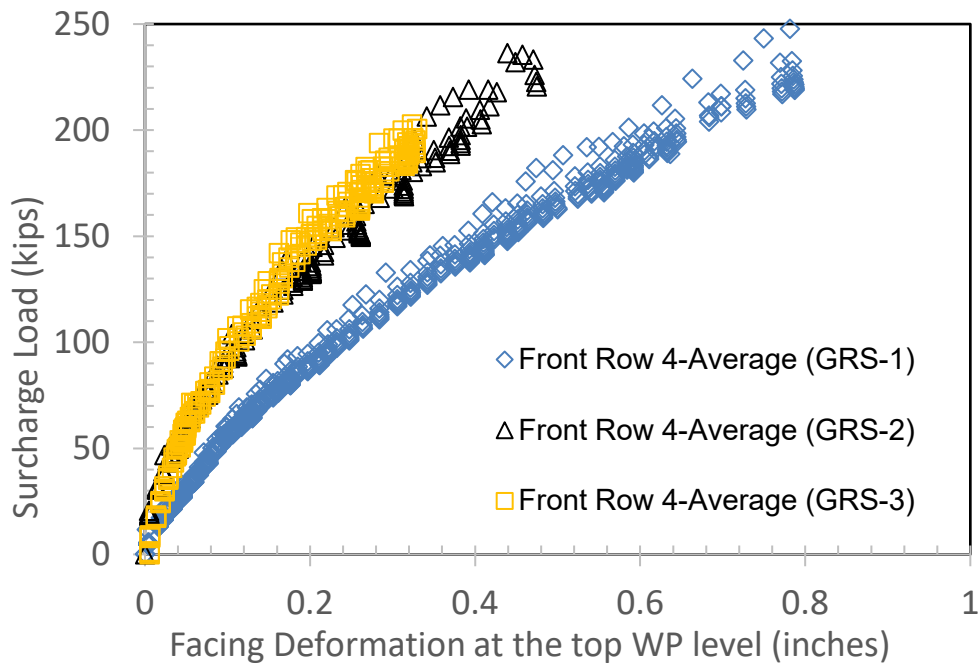

Figure 16. Facing deformation results at the top WP level (Row #4) during surcharge load testing of GRS Models #1 - #3. Deformation values shown are mean values from two WPs at the same elevation

Results in **Figure 17** show the importance of adequate compaction in controlling the later deformation of GRS abutments. All models whose results are shown in this figure were built with CMU blocks, similar to Model #1. However, increased compaction effort in comparable Models #4 and #5 resulted in significantly smaller lateral deformations in these models (e.g. 0.19 in. and 0.14 in., respectively at 200 kips of surcharge load) as compared to that in the control model (i.e. 0.63 in. at 200 kips in Model #1). In comparison, facing deformations of Models #2 and #3 with large facing blocks but with reduced compaction effort were approximately 0.33 inches.
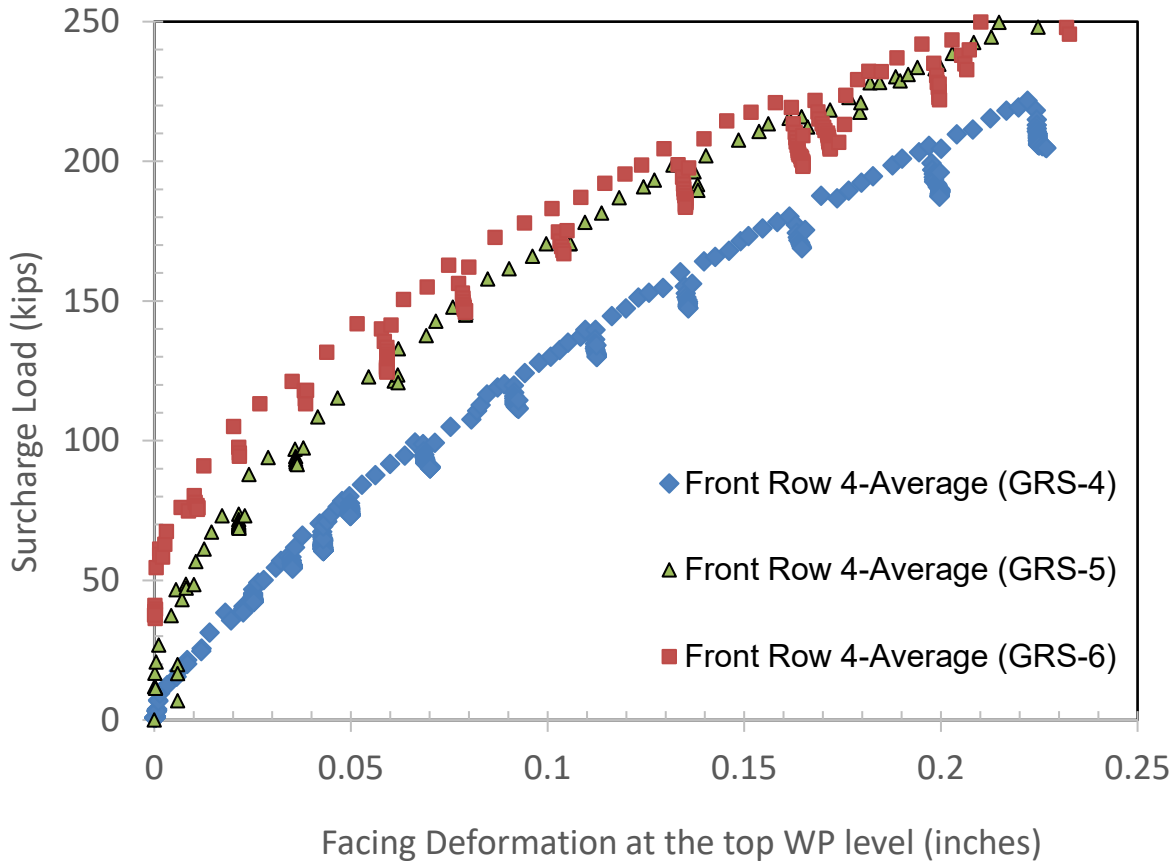

Figure 17. Facing deformation results at the top WP level (Row #4) during surcharge load testing of GRS Models #4 - #6. Deformation values shown are mean values from two WPs at the same elevation

c. Vertical earth pressures

Figure 18 shows measured vertical pressure at mid-height (~44-47 in. above foundation level) within the abutment (**Figure 4**). Results show that vertical pressure in the backfill increased essentially linearly and proportional to the surcharge load applied at the

abutment surface throughout the loading period. Data in **Figure 18** also show that results for the models with large facing blocks are consistent and essentially identical to each other. The results for the CMU facing (Model #1) track those for Models #2 and #3 closely but show slightly greater magnitudes throughout the test. This difference could be due to differences in the quality of compaction in these models where a better compacted column of soil above the EPC in the case of large-block models may have been able to interlock better with the surrounding soil and bridge over the EPC, resulting in somewhat lower vertical pressures applied to, and measure by, the sensor at that location.
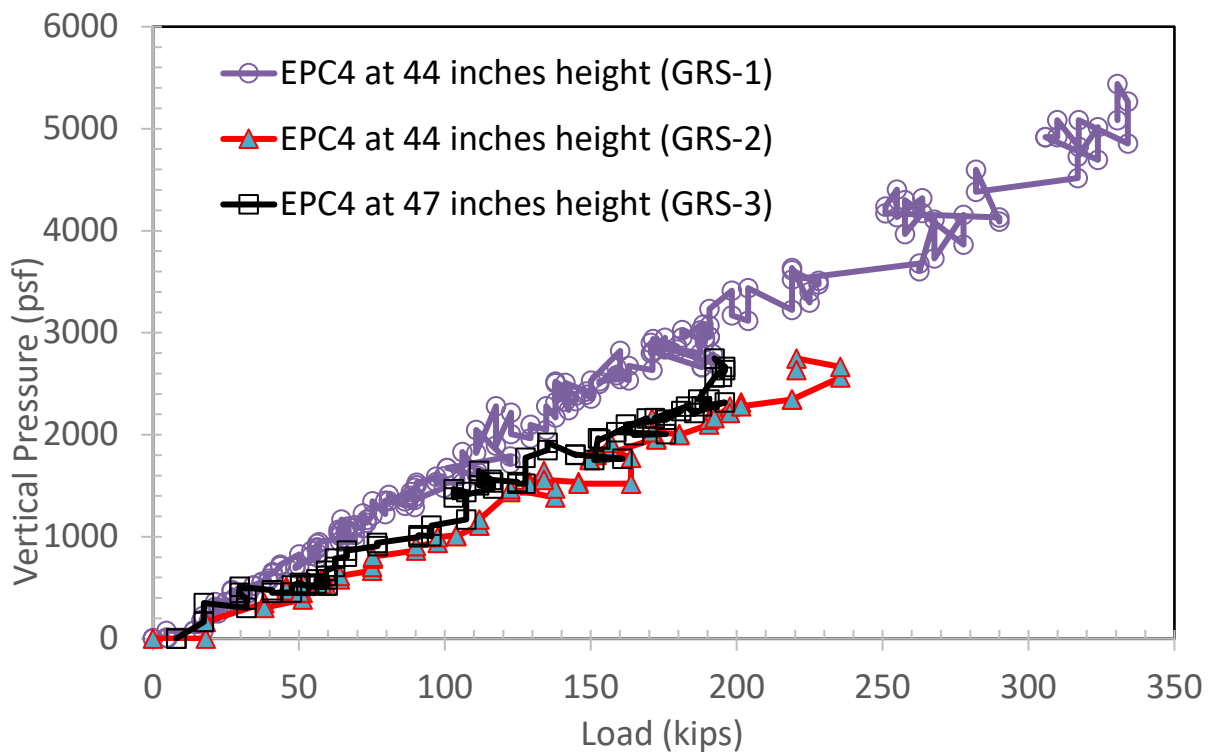

Figure 18. Variations of vertical pressure at mid-height of GRS abutment models as a function of surcharge load

d. Construction time and labor requirements

Figure 19 shows a comparison of cumulative construction times in person-hours for the six GRS models investigated in this study. The flat line at the end of the GRS Model #1 construction is the in-filling of top three rows of CMU blocks across the abutment facing with rebar and concrete for added stability based on FHWA guidelines. This process is not applicable to the solid large-blocks used in Model #2 and #3. Results show that the

construction of GRS Model #3 with large-block facing and increased (i.e. 12") reinforcement spacing was significantly faster than that of GRS Model #1 (CMU block facing with reinforcement layers placed at every 8"), i.e. (~55% shorter construction time) and 33% shorter than that for GRS Model #2 (large block facing with reinforcement layers placed at every 8"). This is a significant practical outcome, which both confirms and quantifies one of the main advantages of large-block GRS abutment alternatives that had been postulated in this project.

In-filling of top three rows of CMU blocks across the abutment facing (with rebar and concrete) for added stability (FHWA guidelines) - Not applicable to the solid large-blocks used in Model #2 and #3
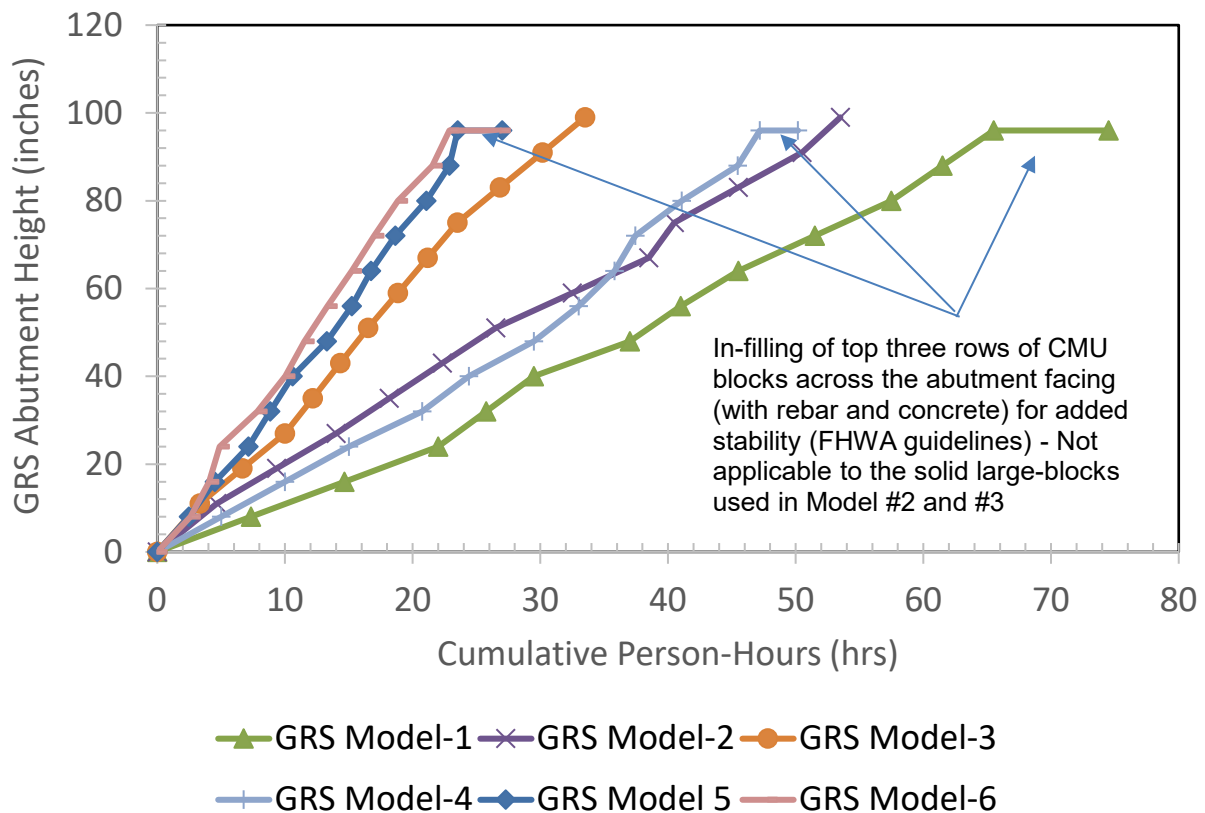
Figure 19. Comparison of construction time (in person-hours) between GRS Abutment Models #1-#6

Results also show that subsequent models that were nominally identical to the control model were built at increasingly faster rate during the project (i.e. Models #4 and #5 vs. Model #1). This demonstrates in quantitative terms that as the team became more familiar with the construction sequence and procedure for the GRS abutment models, the amount of time needed to build each model abutment became increasingly and consistently shorter than those of the previous models including those built with large blocks and reduced compaction effort. This also constitutes a finding with significant practical implications for counties, cities and other stakeholders indicating that as these

entities build more GRS-IBS projects across different states, these systems become even more cost competitive and less disruptive of local traffic over time.

13. Performance of field GRS bridge abutments

In collaboration with ODOT's Materials Division (Mr. Scott Garland, PE) and survey crew, data were collected on abutment movements of three recent GRS bridges in Caddo County: 1) East Cache Creek, 2) Two Hatchet Creek, and 3) Little Washita River (**Figure 20 through 22-** Photographs courtesy of Tom Simpson, PE). The Little Washita River bridge abutments were built using large solid concrete blocks (2' × 2' × 4') as the first GRS-IBS of its kind in Oklahoma. Construction documents for these bridges are available at the BIA regional office in Anadarko, OK (Mr. Tom Simpson, PE). Latest survey data on these bridges are shown in **Figures 23 through 25.**

Survey results to date indicate that all three GRS-IBS projects show essentially uniform settlement across the width of their abutments and between their two abutments over the survey period (which is approximately 1.5 years in the cases of East Cache Creek and Two Hatchet Creek bridges). As a result, the magnitudes of settlement to date, while are somewhat larger than the FHWA recommended limit of 1 inch, have not resulted in any visible problems or serviceability issues, and all bridged have been reported to perform very well. This is considering the fact that these bridges have experienced significant amount of precipitation and flooding periods after construction.

Figure 20. Recently constructed East Cache Creek (CMU block facing) GRS-IBS in Caddo County, OK

Figure 21. Recently constructed Two Hatchet Creek (CMU block facing) GRS-IBS in Caddo County, OK

Figure 22. Recently constructed Little Washita River (Large block facing) GRS-IBS in Caddo County, OK
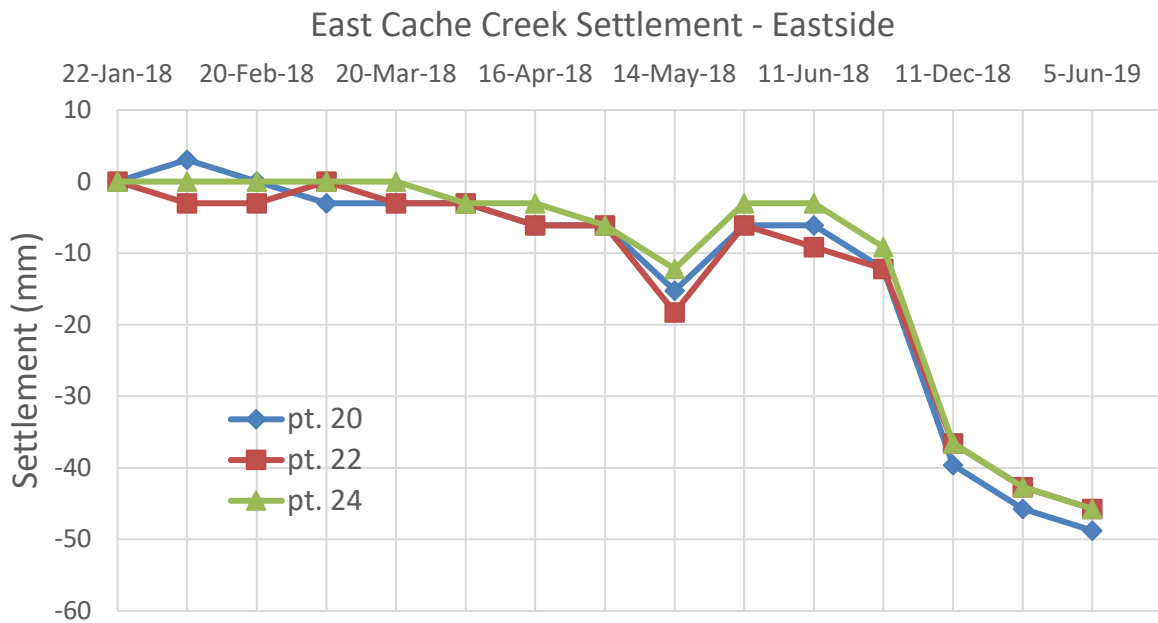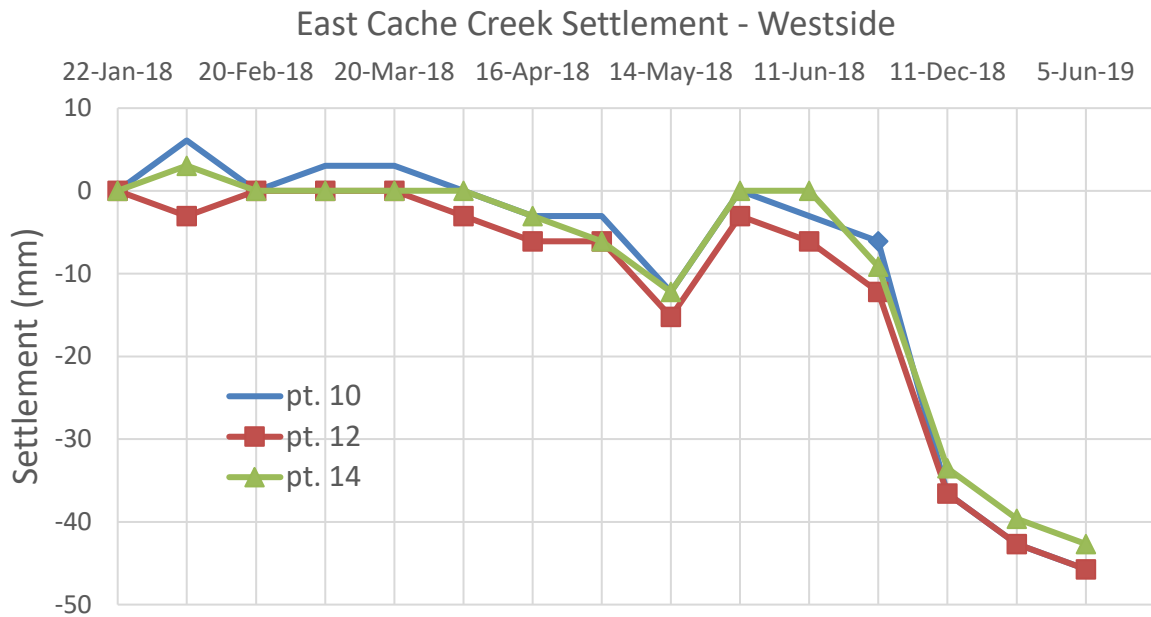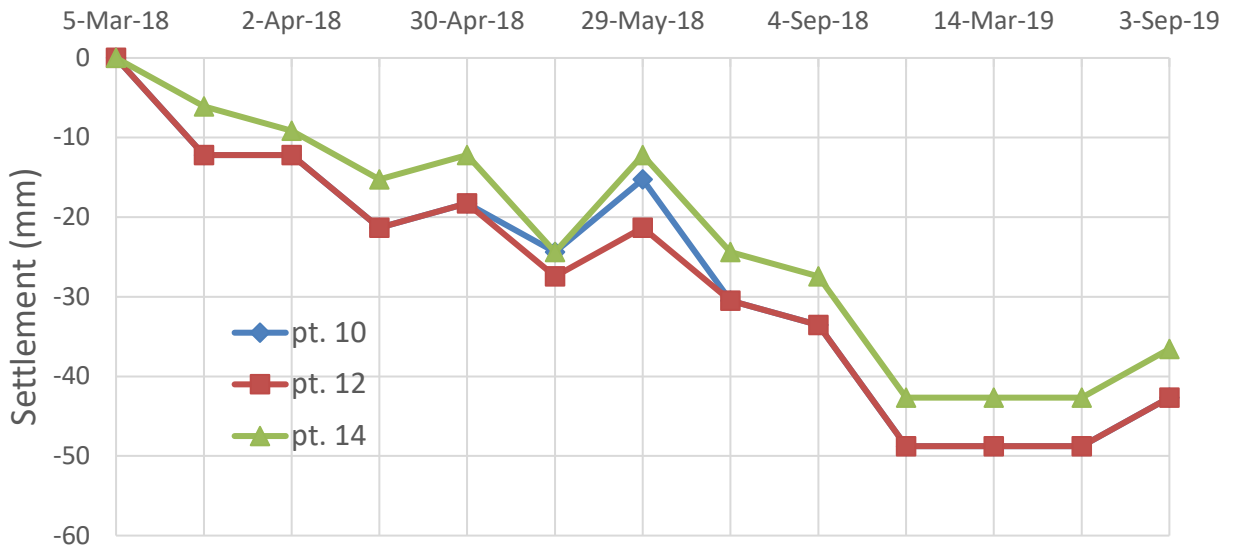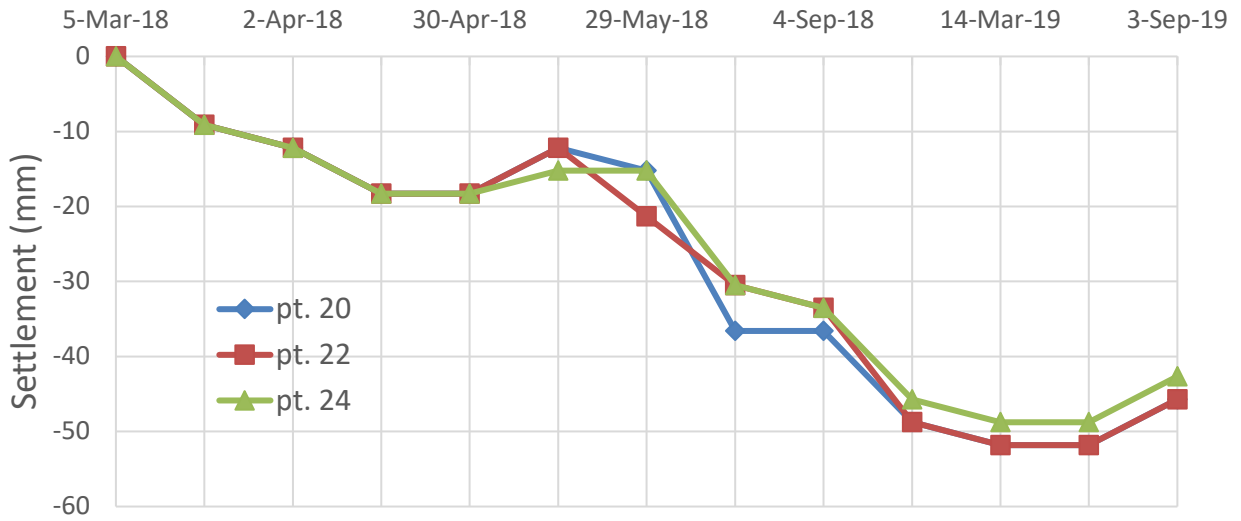
Figure 23. (Top) Measured settlements of the East Cache Creek Bridge at its GRS abutment locations Westside; (Bottom) Eastside (numbered survey points indicated are located on the corners and the middle across the bridge abutment width on each side)

Figure 24. (Top) Measured settlements of the Two Hatchet Creek Bridge at its GRS abutment locations Westside; (Bottom) Eastside (numbered survey points indicated are located on the corners and the middle across the bridge abutment width on each side)
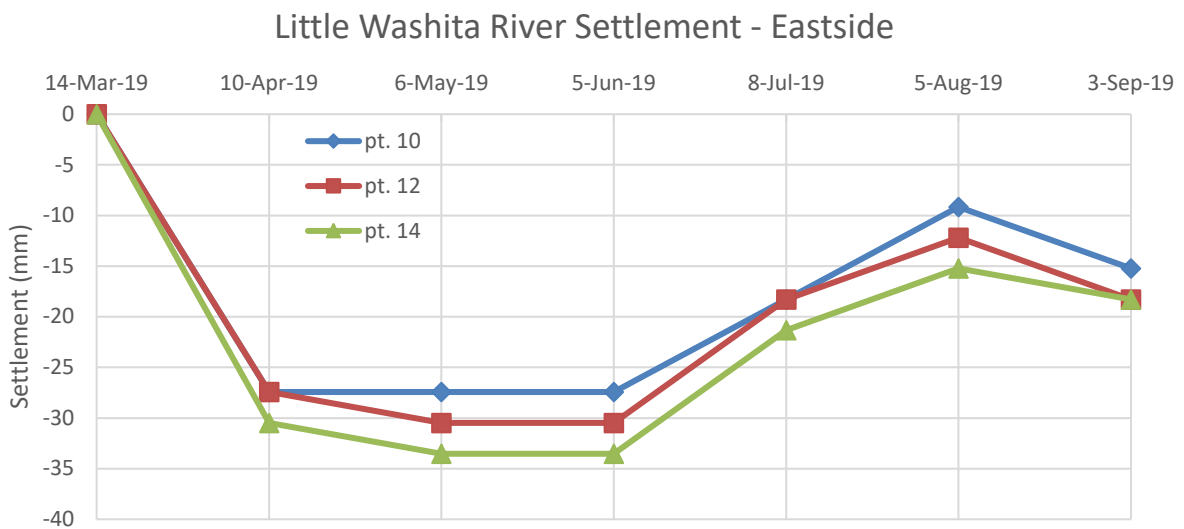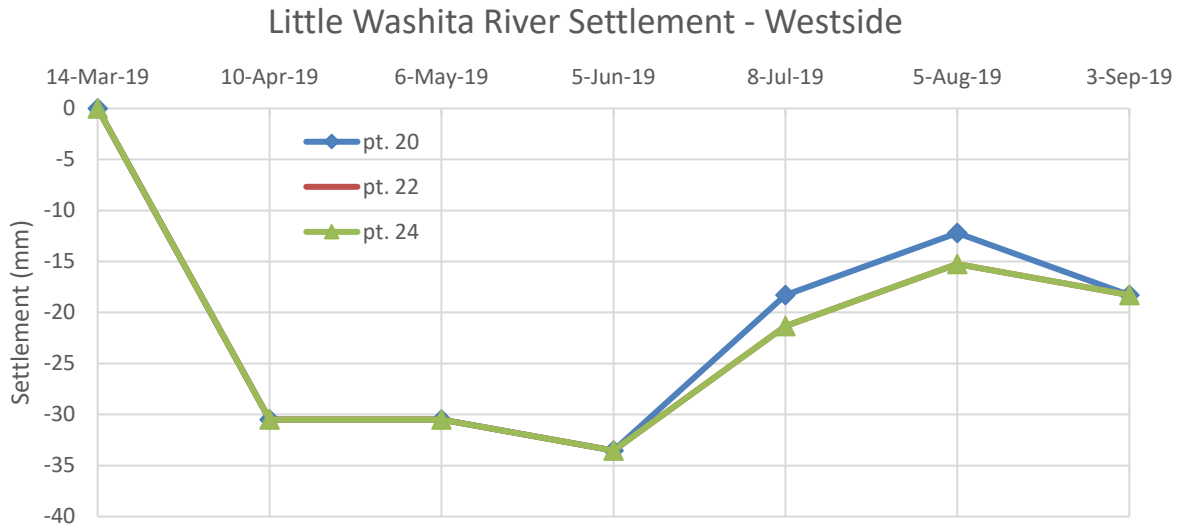
Figure 25. (Top) Measured settlements of the Little Washita River Bridge at its GRS abutment locations Westside; (Bottom) Eastside (numbered survey points indicated are located on the corners and the middle across the bridge abutment width on each side)

Conclusions

A set of six instrumented full-scale (8 ft-high) GRS abutment models was constructed and load tested at an outdoor test station in order to study the influences of facing type, reinforcement spacing, fill aggregate and compaction effort on the structural performance and construction speed of GRS bridge abutments in the field. Different GRS models examined included open-graded and dense-graded aggregates, hollow concrete masonry units (CMU) and larger (i.e. 24" × 24" × 48") solid concrete blocks, 8-in. and 12-in. reinforcement spacing, and reduced vs. recommended compaction efforts.

Results of the study showed that use of large concrete facing blocks instead of CMU can indeed improve both the structural performance and construction speed of GRS bridge abutments. Models with large-block facing tested in this study (i.e. Models #2 and #3) were easier to compact during construction and consistently showed smaller deformations relative to the otherwise identical control model (Model #1).

The influence of backfill compaction on the structural performance of GRS abutments was also demonstrated and quantified. It was shown that models built using recommended compaction effort (i.e. Models #4 and #5) showed significantly smaller settlements and facing lateral deformations under the surcharge load when compared to the control model that had been built with reduced compaction effort (Model #1).

It was also observed that repeat construction of GRS abutments by the research team during the course of this project led to faster construction of subsequent model abutments. The practical implication of this finding is that widespread adoption and more frequent construction of GRS-IBS projects by the counties and cities across the state can lead to further cost savings and reduced traffic disruptions due to shorter construction periods.

Finally, regular survey of three recent GRS-IBS projects in Caddo County, OK during the period of this project has shown that all three bridges have performed very well with no sign of differential settlements or other serviceability problems. One of these GRS bridges was built using the same large concrete blocks that were used in the full-scale tests reported in this study and constitutes the first large-block-facing GRS-IBS in Oklahoma. Results of this study have provided further verification that GRS-IBS projects can indeed serve as viable and cost-effective solutions for the reconstruction or replacement of numerous local and county bridges that are functionally obsolete or structurally deficient relative to the current stability and performance requirements.

Acknowledgments

References Cited

Adams, M., Nicks, J., Stabile, T., Wu, J., Schlatter, W., and Hartmann, J., 2012a. Geosynthetic Reinforced Soil Integrated Bridge System Interim Implementation Guide, *Report No. FHWA-HRT-11-026*, Federal Highway Administration, Washington, DC. Available at: http://www.fhwa.dot.gov/publications/research/infrastructure/structures/11026/index.cfm

Adams, M., Nicks, J., Stabile, T., Wu, J., Schlatter, W., and Hartmann, J., 2012b. Geosynthetic Reinforced Soil Integrated Bridge System Synthesis Report, *Report No. FHWA-HRT-11-027*, Federal Highway Administration, Washington, DC.

Adams, M. and Nicks, J., 2018. Design and Construction Guidelines for Geosynthetic Reinforced Soil Abutments and Integrated Bridge Systems, *Report No. FHWA-HRT-17-080*, Federal Highway Administration, Washington, DC.

ASTM C136 / C136M-14, Standard Test Method for Sieve Analysis of Fine and Coarse Aggregates, ASTM International, West Conshohocken, PA, 2014, www.astm.org.

ASTM D698-12e2, Standard Test Methods for Laboratory Compaction Characteristics of Soil Using Standard Effort (12 400 ft-lbf/ft^3 (600 kN-m/m^3)), ASTM International, West Conshohocken, PA, 2012, www.astm.org.

ASTM D1557-12e1, Standard Test Methods for Laboratory Compaction Characteristics of Soil Using Modified Effort (56,000 ft-lbf/ft^3 (2,700 kN-m/m^3)), ASTM International, West Conshohocken, PA, 2012, www.astm.org.

ASTM D3080 / D3080M-11, Standard Test Method for Direct Shear Test of Soils under Consolidated Drained Conditions, ASTM International, West Conshohocken, PA, 2011, www.astm.org.

ASTM D4595-17, Standard Test Method for Tensile Properties of Geotextiles by the Wide-Width Strip Method, ASTM International, West Conshohocken, PA, 2017, www.astm.org.

Chicago Pneumatic, 2011. Safety and operating instructions for Rammer MS 780, https://www.crowderpneumatics.com/assets/files/MS%20780%20Tamper%20Safety%20&%20Operating%20Instructions.pdf.

FHWA 2012, EDC-1 Innovations (2011-2012), https://www.fhwa.dot.gov/innovation/everydaycounts/edc-1.cfm

FHWA 2014, EDC-1 Innovations (2013-2014), https://www.fhwa.dot.gov/innovation/everydaycounts/edc-2.cfm

FHWA 2016, EDC-1 Innovations (2015-2016), https://www.fhwa.dot.gov/innovation/everydaycounts/edc-3.cfm

Hatami K, Pena L, Ngo T and Miller GA, 2017. Feasibility Study of GRS-IBS for Bridge Abutments in Oklahoma. *Final Report No. FHWA-OK-16-07*, ODOT SP&R ITEM NUMBER 2262, ODOT, Oklahoma City, OK, May 2017, 488p.

Hatami K, 2017. Personal Communications with Tom Simpson, PE, BIA Office, Anadarko, OK.